ELSEVIER

Journal of Nuclear Materials 245 (1997) 179–184

journal of nuclear materials

Characterization of U–2 wt% Mo and U–10 wt% Mo alloy powders prepared by centrifugal atomization

Ki Hwan Kim [a,*], Don Bac Lee [a], Chang Kyu Kim [a], Gerard E. Hofman [b], Kyung Wook Paik [c]

[a] *Korea Atomic Energy Research Institute, 150 Dukjin-dong Yusong-gu, Taejon 305-353, South Korea*
[b] *Argonne National Laboratory, 9700 South Cass Avenue, Argonne IL 60439, USA*
[c] *Korea Advanced Institute of Science and Technology, 373-1 Kusong-dong, Yusong-gu, Taejon 305-701, South Korea*

Received 28 October 1996; accepted 31 January 1997

Abstract

The characteristics of high density U–Mo alloy powder solidified rapidly by the centrifugal atomization process have been examined. The results indicate that most of the atomized U–Mo alloy particles have a smooth surface and near-perfect spherical shape. The atomized powder, irrespective of particle size, is found to be single phase γ-U alloy with isotropic structure and non-dendritic grain. The continuous cooling DSC trace of U–2 wt% Mo alloy shows a small, broad endothermic peak originated from the formation of α-U phase and U_2Mo phase, whereas that of U–10 wt% Mo alloy shows no peak over all temperature ranges associated with the decomposition of γ-U phase. The γ-U phase of U–2 wt% Mo powder is decomposed as the α-U phase and the U_2Mo phase after an annealing treatment at 400°C for 100 h. But the γ-U phase of atomized U–10 wt% Mo powder remains as it was.

---

1. Introduction

The conversion from high enriched uranium (HEU) to low enriched uranium (LEU) for use in research reactor fuel requires a large increase in the fissile uranium per unit volume to compensate for the reduction in enrichment. The development of commonly used aluminum-based dispersion fuels using U_3Si_2 as the fuel component has been rather successful in converting reactors requiring fuel element loadings of up to about 5 g U cm^{-3} [1–3]. U_3Si_2 is found to possess very stable irradiation behavior, but the difficulties in rolling fuel meat do not allow loading higher than ~ 6 g U cm^{-3} [4,5]. Attempts to use higher-density uranium compounds have proved unsuccessful [2]. While the vast majority of reactors can be satisfactorily operated with U_3Si_2–Al dispersion fuel, several high performance reactors require loadings even up to $8 \times 10–9 \times 10$ g U cm^{-3}.

Consequently, in the renewed fuel development program of the Reduced Enrichment for Research and Test Reactors (RERTR) Program, attention has shifted to high density uranium alloys. Early irradiation experiments with uranium alloys showed promise of acceptable irradiation behavior if these alloys could be maintained in their cubic γ-U crystal structure [6]. Alloys with tendency to form this gamma phase are: U–Cr, U–Mo, U–Nb, U–Re, U–Ru, U–Ti, U–V, U–Zr, etc. Among these, the alloy which has a relatively large range of gamma phase is found to be U–Mo. In addition Mo has a relatively low neutron caption cross-section. Below 560°C the stable structure of U–Mo alloys is a mixture of α-U and γ′ phase (U_2Mo) as shown in Fig. 1 [7]. However, by rapid cooling from the gamma phase, U–Mo alloy easily retains this phase in a metastable state. If this metastable gamma phase can be maintained during fuel element fabrication and irradiation and if the alloy has good compatibility with aluminum

---

[*] Corresponding author. Tel.: +82-42 868 2308; fax: +82-42 868 8346.

PII S0022-3115(97)00011-1

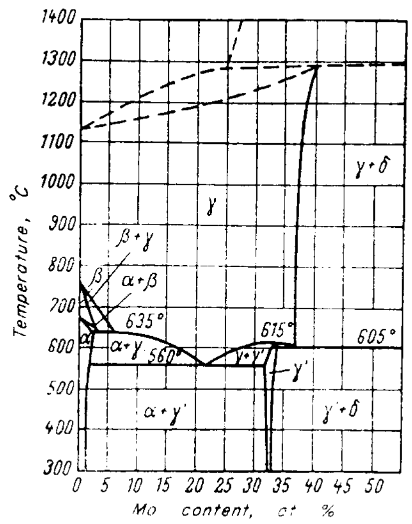

Fig. 1. Uranium–molybdenum phase.

matrix, U–Mo alloy would be a prime candidate for dispersion fuel for research reactors. In this study U–2 wt% Mo and U–10 wt% Mo powder were prepared by rotating disk centrifugal atomization and were characterized for application as a dispersant for research reactor fuel elements.

2. Experimental procedure

A proportioned charge of depleted uranium lumps with purity 99.9% and molybdenum buttons with purity 99.7% was induction-melted in a graphite crucible coated with a high-temperature-resistant ceramic. The molten metal was fed through an orifice onto a rotating graphite disk in an argon atmosphere. In order to obtain the desired size distribution and shape, the atomization parameters were adjusted [8,9]. The atomized powder was collected in a container at the bottom of the funnel shaped chamber. The batch size per each run of particle production was approximately 4 kg in mass due to nuclear criticality control in fuel fabrication.

Powder size distribution of the atomized powder was classified by sieve analysis. The density of powder according to particle size was measured by Archimedean immersion method. The morphology and microstructure of the powder according to atomized particle size were characterized with a scanning electron microscope (SEM). Composition analysis was done by energy dispersive spectroscopy (EDS) with the SEM. The phase transformation temperature of the atomized powder was determined using a differential scanning calorimeter (DSC); generally the rate of temperature increase was chosen as 20°C min^{-1}. The alloy phases of as-atomized and heat-treated powder were analyzed by X-ray diffraction, using the Cu Kα wave length.

3. Result and discussion

The shape of the atomized U–Mo alloy particles as observed by scanning electron microscope is shown in Fig. 2. Most of the particles have a smooth surface (Fig. 3) and generally near-perfect spherical shape with few attached satellites. On the other hand the fine particles (below 45 μm) produced have a lengthened or flake-like morphology. The action of surface tension force is thought to be the reason why atomized particles have a spherical shape [10,11]. These results correspond with the experimental results by Kato et al. who illustrated the effect of disk materials on the shape of atomized Ni-base superalloy powder [9]. Kato's results showed that atomized particles prepared by a graphite disk with higher thermal conductivity had near-perfect spherical shape, but that those pre-

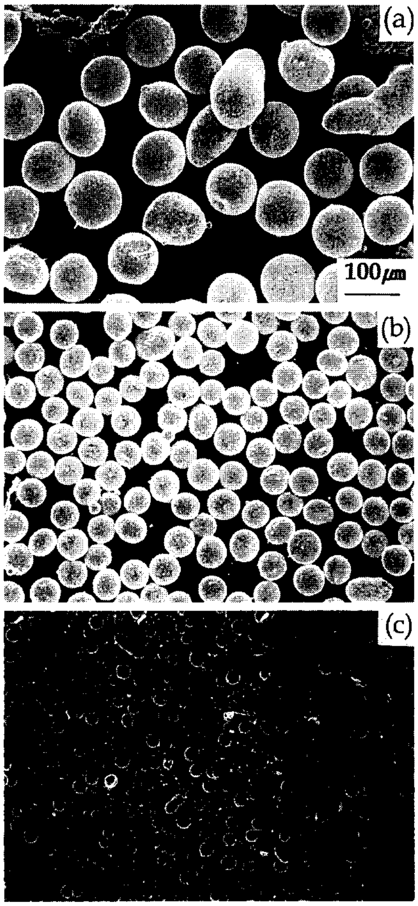

Fig. 2. Photographs showing the shape of atomized U–Mo alloy powder (×100): (a) 120–140 mesh, (b) 200–240 mesh and (c) −325 mesh.

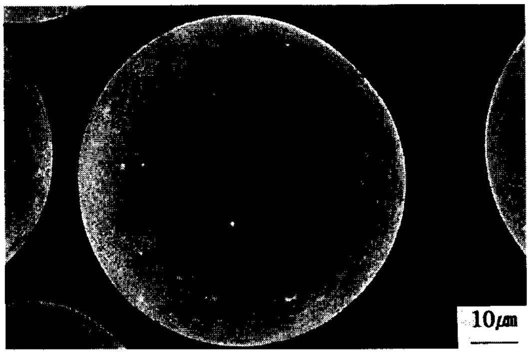

Fig. 3. Photograph showing the surface of atomized alloy powder.

pared by a carbon steel disk and an asbestos disk with lower thermal conductivity had an irregular shape. Because the heat of the melt on the rotating disk is easily removed through graphite with higher thermal conductivity, a frozen layer with a serrated shape is formed in graphite disk edge. Under these circumstances the droplets that are directly separated from the frozen layer edge have the shape of a sphere before its material begins to solidify. The spherical particle then completely solidifies and its collision with an atomization chamber wall does not alter its shape. Hence, the particles would have a tendency to form spherical shape under the action of surface tension force, when the disintegrated droplets maintain a liquid state for the time required for the formation of spherical particles.

Fig. 4 shows the influence of the feed rate of melt on the particle size distribution of atomized U–Mo alloy powder in terms of number fractions. When the feeding rate of melt is small, the particle size distribution displays a bimodal distribution with the main and secondary particles. The secondary particles constitute a small portion of all atomized particles relative to the main particles. Champagne et al. assumed that the bimodal particle size distribution was originated from the direct drop formation mode, which occurred at a relatively small rate of melt feed in the rotating electrode process of iron, steel, copper, aluminum and zinc [12]. However, when the feeding rate becomes large, the particle size distribution displays a mono-modal distribution with the main particles. Such a size distribution has frequently been seen in the ligament disintegration mechanism [13]. It is known that ligament disintegration occurs in the case of large feeding rates of melt in the rotating electrode process. When the feeding rate increases, the dimensions of protuberances around the edge of the disk increase. The larger protuberances stretch into ligaments which eventually break down into strings of many particles at some distance from the edge of the rotating disk. Each protuberance gives birth to a considerable number of particles.

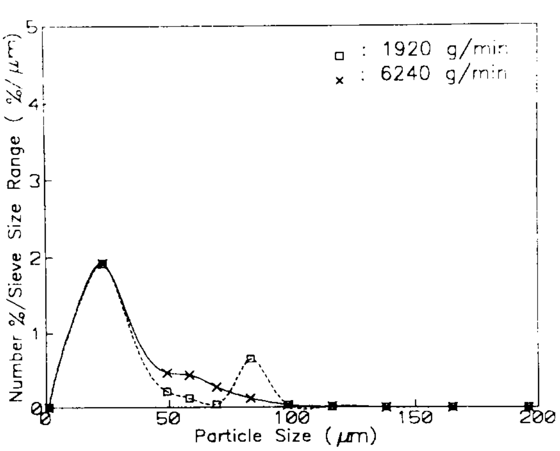

Fig. 4. Influence of the feeding rate of melt on the particle size distribution of atomized powder.

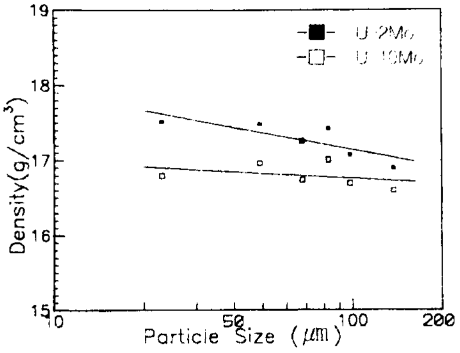

Fig. 5. Variation of density according to particle size in the atomized U–Mo alloy powder.

Fig. 5 shows the particle density versus particle size. The average densities of U–2 wt% Mo and U–10 wt% Mo are about 17.3 and 16.8 g/cm^3, respectively. Irrespective of alloy composition, the density of atomized U–Mo powder is found to decrease as the particle size increases. This is due to the increasing amount of internal pores, as shown in Fig. 6. Scanning electron microscopy reveals that a few of the centrifugal atomization particles contain large spherical pores in their centers, created during the liquid drop

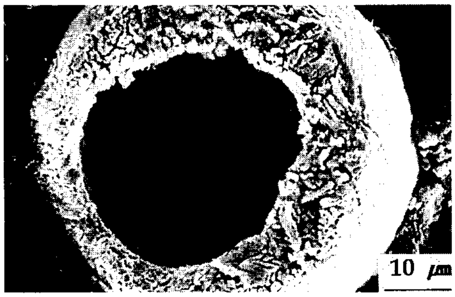

Fig. 6. Photograph showing the pore of atomized U–Mo alloy powder.

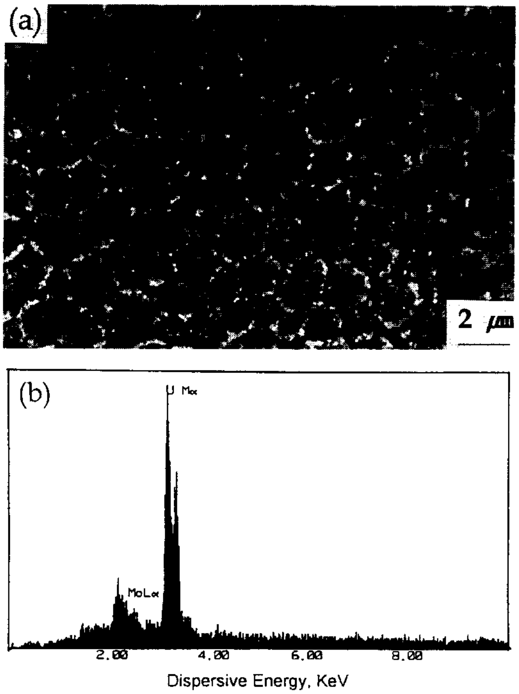

Fig. 7. (a) Micrograph of atomized U–2 wt% Mo powder and (b) energy dispersive spectra from its matrix.

formation. The volume fraction of internal pores is thought to increase with powder size, because the larger droplets have a greater tendency to trap cooling gas while separating from the disk [14].

The cross-sectional micrographs of atomized U–2 wt% Mo and U–10 wt% Mo alloy particles, with the EDS analysis results, are illustrated in Figs. 7 and 8. It is seen that the microstructure of both types of atomized particles is polycrystalline, with many non-dendritic γ-U grains below 5 μm in size. The grain size becomes smaller as the particle size becomes finer. This suggests a more-rapid cooling of finer powder owing to the increase of the specific surface area. Because the cooling rate of the finer drop is higher, the time available for solidification decreases and the tendency to form finer polycrystallines enhances. Despite the rapid solidification, the SEM images reveal some Mo segregation, or cored microstructure, characteristic of an alloy with a substantial liquidus–solidus gap, such as U–Mo alloy. Also, EDS shows that the matrix of U–10 wt% Mo particle is more supersaturated with Mo than that of U–2 wt% Mo particle. At extremely high rates of solidification (~ 100 cm/s), microsegregation-free alloys may be produced by solute trapping [15]. However, the U–Mo powder prepared by centrifugal atomization does not impose such high growth rates and shows microsegregation, especially in U–10 wt% Mo alloy.

The X-ray diffraction patterns of atomized U–2 wt% Mo and U–10 wt% Mo alloy powders are shown in Fig. 9.

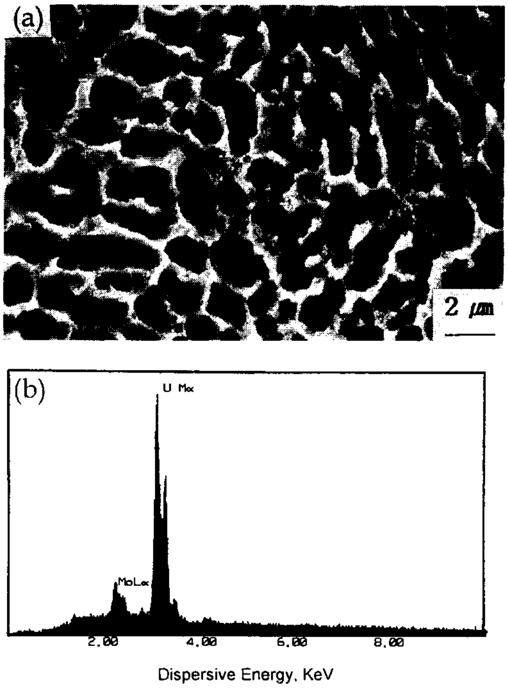

Fig. 8. (a) Micrograph of atomized U–10 wt% Mo powder and (b) energy dispersive spectra from its matrix.

All phases of atomized alloy powders below 150 μm are found to be the isotopic-metastable γ-U (bcc) phase. It is known that U–2 wt% Mo and U–10 wt% Mo alloy frozen

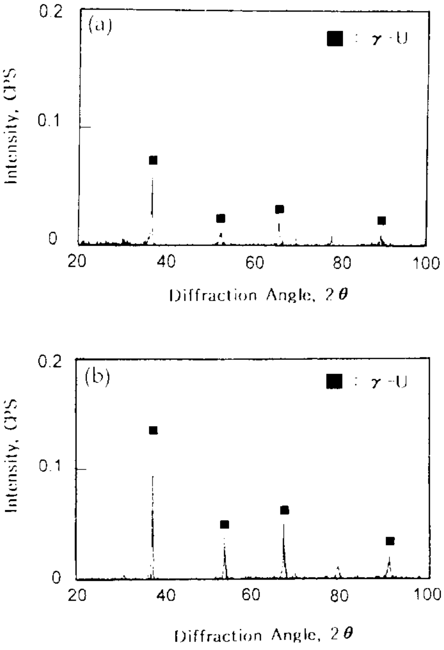

Fig. 9. X-ray diffraction patterns of atomized U–Mo powders: (a) U–2 wt% Mo and (b) U–10 wt% Mo.

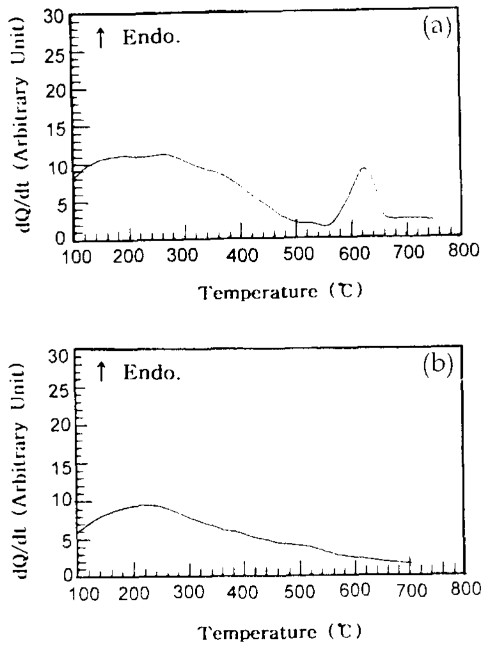

Fig. 10. DSC curves of atomized U–Mo powders during continuous heating: (a) U–2 wt% Mo and (b) U–10 wt% Mo.

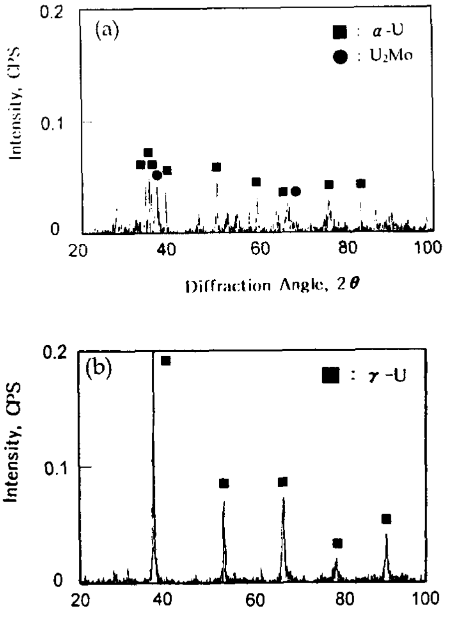

Fig. 11. X-ray diffraction patterns of atomized U–Mo powders after annealing at 400°C for 100 h; (a) U–2 wt% Mo and (b) U–10 wt% Mo.

slowly consist of α-U phase and γ′-U_2Mo intermetallic compound with lamellar structure [7], however γ-U (bcc) phase, which is the equilibrium phase above about 560°C, can be retained in a metastable state at room temperature by rapid solidification. Fig. 10 shows a DSC trace of atomized U–Mo powder during continuous heating to 750°C at a rate of 20°C min^{-1}. The continuous heating DSC trace of U–2 wt% Mo alloy shows a large, broad endothermic peak at about 600°C associated with the decomposition of metastable γ-U. X-ray diffraction of U–2 wt% Mo powder after the continuous heating shows that the γ-U phase of U–2 wt% Mo alloy is decomposed as the α-U phase. The continuous heating DSC trace of U–10 wt% Mo alloy shows no peak over the temperature range originated from the decomposition of γ-U. X-ray diffraction of U–10 wt% Mo powder after the continuous heating demonstrates that the alloy powder remains as the metastable γ-U (bcc) phase. X-ray diffraction patterns and scanning electron micrographs of the atomized U–Mo powders after annealing for 100 h at 400°C are shown in Figs. 11 and 12, respectively. The γ-U phase of U–2 wt% Mo alloy is decomposed as the α-U phase and the γ′-U_2Mo after an annealing, but the γ-U phase of U–10 wt% Mo alloy remains as it was. The γ-U phase of U–2 wt% Mo alloy below the eutectoid temperature (560°C) tends to be decomposed as the thermodynamically stable lamellar structure including α-U and γ′ phase (U_2Mo) [7]. It is known that this reaction is nucleated primarily at γ-U grain boundary and γ-U in the grains is decomposed as α-U and γ-U with higher Mo content rather than γ′ as

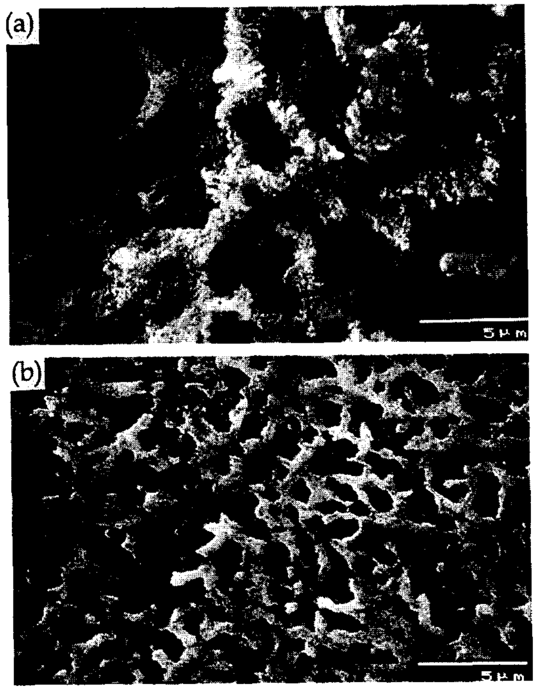

Fig. 12. Scanning electron micrographs of U–Mo powders after annealing at 400°C for 100 h (×5000); (a) U–2 wt% Mo and (b) U–10 wt% Mo.

would be expected for normal eutectoid reactions [16,17]. Thereafter, the matrix is transformed again by so-called low temperature mechanism, with which decomposition is initiated by the formation of ordered γ'. Consequently, transformation occurs continuously involving the formation of an ordered intermediate phase (γ'), with α-U presumably forming from a solute depleted matrix around grain boundary. On the other hand, the scanning electron micrograph for the U–10 wt% Mo powder annealed at 400°C for 100 h illustrates that U–10 wt% Mo powder still reveals fine grain structure below 5 μm in size with microsegregation of Mo. It is thought that these results originated from the supersaturation of Mo in the metastable γ-U solid solution of U–10 wt% Mo alloy. Large substitution of Mo atom within the U matrix causes U atoms to become immobile due to Mo with low diffusivity [18]. Therefore, this confirms that the γ-U phase of atomized U–10 wt% Mo powder can be retained for extended times, presumably because the diffusion-controlled transformation is retarded at increased Mo content.

4. Conclusions

In order to develop nuclear fuel with high uranium density by using isotropic alloy with γ-U phase, high density U–Mo alloy powders are produced by a rotating disk centrifugal atomization method. The characteristics of the atomized alloy powders investigated are as follows:

(1) The size distribution of atomized U–Mo alloy powder shows a relatively narrow distribution. Most of the atomized U–Mo alloy particles have near-perfect spherical shape.

(2) The atomized powder irrespective of particle size is found to be a single phase γ-U alloy with isotropic structure and non-dendritic grain.

(3) The continuous cooling DSC trace of U–2 wt% Mo alloy shows a small, broad endothermic peak originated from the formation of α-U phase. However, the continuous cooling DSC trace of U–10 wt% Mo alloy shows no peak over the temperature range associated with decomposition of γ-U solid solution.

(4) The γ-U phase of atomized U–2 wt% Mo powder is mainly decomposed as the α-U phase and the U_2Mo after annealing at 400°C for 100 h. But the γ-U phase of atomized U–10 wt% Mo powder remains as it was.

Acknowledgements

We would like to acknowledge the support of the work by H.S. Ahn, S.J. Jang and Dr J.M. Park. Thanks are also due to Dr G.L. Snelgrove of Argonne National Laboratory and Dr I.H. Kuk of Korea Atomic Energy Research Institute for considerate comments.

References

[1] S. Nazaré, J. Nucl. Mater. 124 (1984) 14.
[2] G.L. Hofman, J. Nucl. Mater. 140 (1986) 256.
[3] R.C. Birther, C.W. Allen, L.E. Rehn, G.L. Hofman, J. Nucl. Mater. 152 (1988) 73.
[4] J.P. Durand, Proc. 19th Int. Meeting on Reduced Enrichment for Research and Test Reactors, Paris, 1995.
[5] J.P. Durand, P. Laudamy, K. Richer, Proc. 18th Int. Meeting on Reduced Enrichment for Research and Test Reactors, Williamsburg, USA, 1994.
[6] G.L. Hofman, L.C. Walters, in: Materials Science and Technology, Vol. 10A, Nuclear Materials, ed. B.R.T. Frost (VCH, New York, 1994).
[7] Konobeevskin et al., Proc. 2nd Int. Conf. on the Peaceful Uses of Atomic Energy, Geneva, 1958.
[8] I.H. Kuk, C.K. Kim, C.T. Kim, 'Uranium–silicide dispersion fuel utilizing rapid solidification by atomization', US patent no. 4,997,477 (1991).
[9] T. Kato, K. Kusaka, Mater. Trans. JIM. 31 (1990) 362.
[10] T. Kato, K. Kusaka, A. Horata, J. Ichikawa, Tetsuto-to-Hagané 6 (1985) 719.
[11] L.K. Druzhinin, B.V. Safronov, Met. Powder Rep. 38 (1983) 447.
[12] B. Champagne, R. Angers, Powder Metall. Int. 16 (1984) 125.
[13] B. Champagne, R. Angers, Mod. Dev. Powder Metall. 12 (1980) 83.
[14] J.E. Flinn, G.R. Smolik, J. Mater. Sci. Eng. A124 (1990) 39.
[15] W.J. Boettinger, S.R. Coriell, R.F. Sekera, Mater. Sci. Eng. 65 (1984) 27.
[16] H.E. Cook, Acta Metall. 21 (1973) 1445.
[17] G.D. Sandrock, J.A. Perkins, R.F. Struyve, Scr. Metall. 6 (1972) 507.
[18] K.H. Eckelmeyer, in: Microstructural Structure, Vol. 7, ed. McCall (Fallen, 1977).